

CERN-PH-EP-2014-169
15 July 2014

Event-by-event mean p_T fluctuations in pp and Pb–Pb collisions at the LHC

The ALICE Collaboration*

Abstract

Event-by-event fluctuations of the mean transverse momentum of charged particles produced in pp collisions at $\sqrt{s} = 0.9, 2.76$ and 7 TeV, and Pb–Pb collisions at $\sqrt{s_{NN}} = 2.76$ TeV are studied as a function of the charged-particle multiplicity using the ALICE detector at the LHC. Non-statistical fluctuations are observed in all systems. The results in pp collisions show little dependence on collision energy. The Monte Carlo event generators PYTHIA and PHOJET are in qualitative agreement with the data. Peripheral Pb–Pb data exhibit a similar multiplicity dependence as that observed in pp. In central Pb–Pb, the results deviate from this trend, featuring a significant reduction of the fluctuation strength. The results in Pb–Pb are in qualitative agreement with previous measurements in Au–Au at lower collision energies and with expectations from models that incorporate collective phenomena.

*See Appendix A for the list of collaboration members

1 Introduction

The study of event-by-event fluctuations was proposed as a probe of the properties of the hot and dense matter generated in high-energy heavy-ion collisions [1, 2, 3, 4, 5, 6, 7, 8, 9]. The occurrence of a phase transition from the Quark-Gluon Plasma to a Hadron Gas or the existence of a critical point in the phase diagram of strongly interacting matter may go along with critical fluctuations of thermodynamic quantities such as temperature. This could be reflected in non-statistical event-by-event fluctuations of the mean transverse momentum ($\langle p_T \rangle$) of final-state charged particles.

Event-by-event $\langle p_T \rangle$ fluctuations have been studied in nucleus-nucleus (A–A) collisions at the Super Proton Synchrotron (SPS) [10, 11, 12, 13, 14] and at the Relativistic Heavy-Ion Collider (RHIC) [15, 16, 17, 18, 19, 20], where non-statistical fluctuations have been observed. Fluctuations of $\langle p_T \rangle$ were found to decrease with collision centrality, as generally expected in a dilution scenario caused by superposition of partially independent particle-emitting sources. In detail, however, deviations from a simple superposition scenario have been reported. In particular, with respect to a reference representing independent superposition – i.e. a decrease of fluctuations according to $\langle dN_{\text{ch}}/d\eta \rangle^{-0.5}$, where $\langle dN_{\text{ch}}/d\eta \rangle$ is the average charged-particle density in a given interval of collision centrality and pseudorapidity (η) – the observed fluctuations increase sharply from peripheral to semi-peripheral collisions, followed by a shallow decrease towards central collisions [18]. A number of possible mechanisms have been proposed to explain this behavior, such as string percolation [21] or the onset of thermalization and collectivity [22, 23], but no strong connection to critical behavior could be made. It was recently suggested [24, 25] that initial state density fluctuations [26] could affect the final state transverse momentum correlations and their centrality dependence.

Fluctuations of $\langle p_T \rangle$ arise from many kinds of correlations among the p_T of the final-state particles, such as resonance decays, jets, or quantum correlations. To account for these contributions from conventional mechanisms similar studies can be performed in pp, where such correlations are also present. The results from pp could thus be used to construct a model-independent baseline to search for non-trivial fluctuations in A–A which manifest themselves in a modification of the fluctuation pattern with respect to the pp reference.

In this paper, we present results of a multiplicity-dependent study of event-by-event $\langle p_T \rangle$ fluctuations of charged particles in pp collisions at $\sqrt{s} = 0.9, 2.76$ and 7 TeV, and Pb–Pb collisions at $\sqrt{s_{\text{NN}}} = 2.76$ TeV measured with ALICE at the LHC. The experimental data are compared to different Monte Carlo (MC) event generators.

2 ALICE detector and data analysis

The data used in this analysis were collected with the ALICE detector at the CERN Large Hadron Collider (LHC) [27] during the Pb–Pb run in 2010 and the pp runs in 2010 and 2011.

For a detailed description of the ALICE apparatus see [28]. The analysis is based on 19×10^6 Pb–Pb events at $\sqrt{s_{\text{NN}}} = 2.76$ TeV, and 6.9×10^6 , 66×10^6 and 290×10^6 pp events at $\sqrt{s} = 0.9, 2.76$ and 7 TeV, respectively. The standard ALICE coordinate system is used, in which the nominal interaction point is the origin of a right-handed Cartesian coordinate system. The z -axis is along the beam pipe, the x -axis points towards the center of the LHC, φ is the azimuthal angle around the z -axis and θ is the polar angle with respect to this axis. The detectors in the central barrel of the experiment are operated inside a solenoidal magnetic field with $B = 0.5$ T. About half of the Pb–Pb data set was recorded with negative ($B_z < 0$) and positive ($B_z > 0$) field polarity, respectively.

A minimum bias (MB) trigger condition was applied to select collision events. In pp, this trigger was defined by at least one hit in the Silicon Pixel Detector (SPD) or in one of the two forward scintillator systems VZERO-A ($2.8 < \eta < 5.1$) and VZERO-C ($-3.7 < \eta < -1.7$). In Pb–Pb, the MB trigger

46 condition is defined as a coincidence of hits in both VZERO detectors.

47 In this analysis, the Time Projection Chamber (TPC) [29] is used for charged-particle tracking in $|\eta| <$
 48 0.8. In the momentum range selected for this analysis, $0.15 < p_T < 2$ GeV/ c , the momentum resolution
 49 $\sigma(p_T)/p_T$ is better than 2%. The tracking efficiency is larger than 90% for $p_T > 0.3$ GeV/ c and drops to
 50 about 70% at $p_T = 0.15$ GeV/ c .

51 Primary vertex information is obtained from both the Inner Tracking System (ITS) and the TPC. Events
 52 are used in the analysis when at least one accepted charged-particle track contributes to the primary
 53 vertex reconstruction. It is required that the reconstructed vertex is within ± 10 cm from the nominal
 54 interaction point along the beam direction to ensure a uniform pseudo-rapidity acceptance within the
 55 TPC. Additionally, the event vertex is reconstructed using only TPC tracks. The event is rejected if the
 56 z -position of that vertex is different by more than 10 cm from that of the standard procedure.

57 In Pb–Pb, at least 10 reconstructed tracks inside the acceptance are required. The contamination by
 58 non-hadronic interactions is negligible in the event sample that fulfills the aforementioned selection
 59 criteria. The centrality in Pb–Pb is estimated from the signal in the VZERO detectors using the procedure
 60 described in [30, 31].

61 The charged-particle tracks used for this analysis are required to have at least 70 out of a maximum of
 62 159 reconstructed space points in the TPC, and the maximum χ^2 per space point in the TPC from the
 63 momentum fit must be less than 4. Daughter tracks from reconstructed secondary weak-decay topologies
 64 (*kinks*) are rejected. The distance of closest approach (DCA) of the extrapolated trajectory to the primary
 65 vertex position is restricted to less than 3.2 cm along the beam direction and less than 2.4 cm in the
 66 transverse plane. The number of tracks in an event that are accepted by these selection criteria is denoted
 67 by N_{acc} .

68 Event-by-event measurements of the mean transverse momentum are subject to the finite reconstruction
 69 efficiency of the detector. While efficiency corrections can be applied on a statistical basis to derive
 70 the inclusive $\langle p_T \rangle$ of charged particles in a given kinematic acceptance range, such an approach is not
 71 adequate for event-by-event studies. The event-by-event mean transverse momentum is therefore ap-
 72 proximated by the mean value $M_{\text{Ebe}}(p_T)_k$ of the transverse momenta $p_{T,i}$ of the $N_{\text{acc},k}$ accepted charged
 73 particles in event k :

$$M_{\text{Ebe}}(p_T)_k = \frac{1}{N_{\text{acc},k}} \sum_{i=1}^{N_{\text{acc},k}} p_{T,i} . \quad (1)$$

74 Event-by-event fluctuations of $M_{\text{Ebe}}(p_T)_k$ in heavy-ion collisions are composed of statistical and non-
 75 statistical (i.e. *dynamical*) contributions. The two-particle transverse momentum correlator
 76 $C = \langle \Delta p_{T,i} \Delta p_{T,j} \rangle$ is a measure of the dynamical component σ_{dyn}^2 of these fluctuations and therefore
 77 well suited for an event-by-event analysis [13, 18, 32]. The correlator C_m is the mean of covariances of
 78 all pairs of particles i and j in the same event with respect to the inclusive $M(p_T)_m$ in a given multiplicity
 79 class m and is defined as

$$C_m = \frac{1}{\sum_{k=1}^{n_{\text{ev},m}} N_k^{\text{pairs}}} \cdot \sum_{k=1}^{n_{\text{ev},m}} \sum_{i=1}^{N_{\text{acc},k}} \sum_{j=i+1}^{N_{\text{acc},k}} (p_{T,i} - M(p_T)_m) \cdot (p_{T,j} - M(p_T)_m) , \quad (2)$$

80 where $n_{\text{ev},m}$ is the number of events in multiplicity class m , $N_k^{\text{pairs}} = 0.5 \cdot N_{\text{acc},k} \cdot (N_{\text{acc},k} - 1)$ is the number
 81 of particle pairs in event k and $M(p_T)_m$ is the average p_T of all tracks in all events of class m :

$$M(p_T)_m = \frac{1}{\sum_{k=1}^{n_{\text{ev},m}} N_{\text{acc},k}} \sum_{k=1}^{n_{\text{ev},m}} \sum_{i=1}^{N_{\text{acc},k}} p_{T,i} = \frac{1}{\sum_{k=1}^{n_{\text{ev},m}} N_{\text{acc},k}} \sum_{k=1}^{n_{\text{ev},m}} N_{\text{acc},k} \cdot M_{\text{Ebe}}(p_T)_k . \quad (3)$$

82 By construction, C_m vanishes when only statistical fluctuations are present.

83 The results in this paper are presented in terms of the dimensionless ratio $\sqrt{C_m}/M(p_T)_m$ which quantifies
 84 the strength of the non-statistical fluctuations in units of the average transverse momentum $M(p_T)_m$ in
 85 the multiplicity class m .

86 The correlator is computed in intervals of the event multiplicity N_{acc} . In pp collisions, intervals of
 87 $\Delta N_{\text{acc}} = 1$ are used for the calculation of C_m and $M(p_T)_m$. In Pb–Pb collisions, C_m is calculated in the
 88 multiplicity intervals $\Delta N_{\text{acc}} = 10$ for $N_{\text{acc}} < 200$, $\Delta N_{\text{acc}} = 25$ for $200 \leq N_{\text{acc}} < 1000$ and $\Delta N_{\text{acc}} = 100$ for
 89 $N_{\text{acc}} \geq 1000$. To account for the steep increase of $M(p_T)_m$ with multiplicity in peripheral collisions, the
 90 calculation of the correlator in (2) uses values for $M(p_T)_m$ which are calculated in bins of $\Delta N_{\text{acc}} = 1$ for
 91 $N_{\text{acc}} < 1000$. At higher multiplicities, $M(p_T)$ changes only moderately and $M(p_T)_m$ is calculated in the
 92 same intervals as C_m , i.e. $\Delta N_{\text{acc}} = 100$.

93 Additionally, the Pb–Pb data are also analyzed in 5% intervals of the collision centrality. The results
 94 are shown in bins of the mean number of participating nucleons $\langle N_{\text{part}} \rangle$ as derived from the centrality
 95 percentile using a Glauber MC calculation [30]. For the results presented as a function of the mean
 96 charged-particle density $\langle dN_{\text{ch}}/d\eta \rangle$, the mean value $\langle N_{\text{acc}} \rangle$ in each centrality bin is associated with the
 97 measured value for $\langle dN_{\text{ch}}/d\eta \rangle$ from [30]. A linear relation between $\langle N_{\text{acc}} \rangle$ and $\langle dN_{\text{ch}}/d\eta \rangle$ is observed
 98 over the full centrality range, allowing interpolation to assign a value for $\langle dN_{\text{ch}}/d\eta \rangle$ to any interval of
 99 N_{acc} . In pp, $\langle dN_{\text{ch}}/d\eta \rangle$ is calculated for each interval of N_{acc} employing the full detector response matrix
 100 from MC and unfolding of the measured N_{acc} distributions following the procedure outlined in [33].

101 The systematic uncertainties are estimated separately for each collision system (Pb–Pb and pp) and at
 102 each collision energy. The relative uncertainties on $\sqrt{C_m}/M(p_T)_m$ are generally smaller than those on
 103 C_m because most of the sources of uncertainties lead to correlated variations of $M(p_T)_m$ and C_m that tend
 104 to cancel in the ratio $\sqrt{C_m}/M(p_T)_m$. Therefore, all quantitative results shown below are presented in
 105 terms of $\sqrt{C_m}/M(p_T)_m$. The contributions to the total systematic uncertainty on $\sqrt{C_m}/M(p_T)_m$ in pp
 106 and Pb–Pb collisions are summarized in Table 1. Ranges are given when the uncertainties depend on
 107 $\langle dN_{\text{ch}}/d\eta \rangle$ or centrality.

108 The largest contribution to the total systematic uncertainty results from the comparison of $\sqrt{C_m}/M(p_T)_m$
 109 from full MC simulations employing a GEANT3 [34] implementation of the ALICE detector setup [35]
 110 to the MC generator level. Processing the events through the full simulation chain alters the result for
 111 $\sqrt{C_m}/M(p_T)_m$ with respect to the MC generator level by up to 6% in high multiplicity pp collisions. This
 112 includes effects of tracking efficiency dependence on the transverse momentum. The studies in pp are
 113 performed using the Perugia-0 tune of PYTHIA6 [36, 37], similar results are obtained with PHOJET [38].
 114 HIJING [39] is used for Pb–Pb collisions, where the differences are slightly smaller, reaching up to 4%
 115 in most central collisions.

116 These deviations are added to the systematic data uncertainties to allow for a direct comparison of the
 117 experimental results to model calculations on the MC event generator level.

118 Another major contribution to the total systematic uncertainty emerges from the difference between
 119 the standard analysis using only TPC tracks and an alternative analysis employing a hybrid tracking
 120 scheme. The hybrid tracking combines TPC and ITS tracks when ITS detector information is available,
 121 and thus provides more powerful suppression of secondary particles (remaining contamination 4–5%) as
 122 compared to the standard TPC-only tracking ($\sim 12\%$). The TPC, on the other hand, features very stable
 123 operational conditions throughout the analyzed data sets. The differences between the results from the
 124 two analyses reach 5% in $\sqrt{C_m}/M(p_T)_m$.

125 At the event level, minor contributions to the total systematic uncertainty arise from the cut on the max-
 126 imum distance of the reconstructed vertex to the nominal interaction point along the beam axis. In the
 127 standard analysis global tracks that combine TPC and ITS track segments are used for the vertex calcula-
 128 tion. Alternatively, we studied also the results when only TPC tracks or only tracklets from the SPD are

129 used to reconstruct the primary vertex. The effect from using the different vertex estimators is negligible
 130 in Pb–Pb collisions. In pp collisions, this effect is small with the exception of the lowest multiplicity bin,
 131 where it reaches 2% in $\sqrt{C_m}/M(p_T)_m$. Additionally, the cut on the difference between the z -positions
 132 of the reconstructed vertices obtained from global tracks and TPC-only tracks is varied. This shows a
 133 sizable effect only in peripheral Pb–Pb and low-multiplicity pp collisions (2–3% in $\sqrt{C_m}/M(p_T)_m$).

134 In addition, variations of the following track quality cuts are performed: the number of space points per
 135 track in the TPC, the χ^2 per degree of freedom of the momentum fit, and the DCA of each track to the
 136 primary vertex, both along the beam direction and in the transverse plane. Neither of these contributions
 137 to the total systematic uncertainty exceeds 3% in $\sqrt{C_m}/M(p_T)_m$.

Collision system $\sqrt{s_{NN}}$	pp 0.9 TeV	pp 2.76 TeV	pp 7 TeV	Pb–Pb 2.76 TeV
Vertex z -position cut	0–0.5%	<0.1%	<0.1%	0.5–1%
Vertex calculation	0–2%	0.5–2%	0.5–2%	<0.1%
Vertex difference cut	0–1.5%	0–3%	0–2%	0–2%
Min. TPC space points	1.5–3%	1–2%	1–3%	2–3%
TPC χ^2 / d.o.f.	<0.1%	<0.1%	<0.1%	<0.1%
DCA to vertex	1%	1–1.5%	0.5–1%	0.5–1%
B-field polarity	0.5%	0.5%	0.5%	0.5%
Centrality intervals	-	-	-	1–3%
TPC-only vs. hybrid	4%	4%	4%	1–5%
MC generator vs. full sim.	0–6%	0–6%	0–6%	0–4%
Total	4.4–7.7%	4.4–7.6%	4.4–7.9%	4.2–7.4%

Table 1: Contributions to the total systematic uncertainty on $\sqrt{C_m}/M(p_T)_m$ in pp and Pb–Pb collisions. Ranges are given when the uncertainties depend on $\langle dN_{ch}/d\eta \rangle$ or centrality.

138 The difference between the results obtained from Pb–Pb data taken at the two magnetic field polarities
 139 is included into the systematic uncertainties. The effect is small (0.5% in $\sqrt{C_m}/M(p_T)_m$). The corre-
 140 sponding uncertainty in pp is assumed to be the same as in Pb–Pb collisions. Finally, the effect of finite
 141 centrality intervals in Pb–Pb, and the corresponding variation of $M(p_T)$ within these intervals, is taken
 142 into account by including the difference between the analyses in 5% and 10% centrality intervals [30, 31]
 143 into the systematic uncertainty. The total uncertainty on $\sqrt{C_m}/M(p_T)_m$ for each data set was obtained by
 144 adding in quadrature the individual contributions in Table 1.

145 3 Results in pp collisions

146 The relative dynamical fluctuation $\sqrt{C_m}/M(p_T)_m$ as a function of the average charged-particle multiplic-
 147 ity $\langle dN_{ch}/d\eta \rangle$ in pp collisions at $\sqrt{s} = 0.9, 2.76$ and 7 TeV is shown in Fig. 1. The non-zero values
 148 of $\sqrt{C_m}/M(p_T)_m$ indicate significant non-statistical event-by-event $M(p_T)$ fluctuations. The fluctuation
 149 strength reaches a maximum of 12–14% in low multiplicity collisions and decreases to about 5% at the
 150 highest multiplicities. No significant beam energy dependence is observed for the relative fluctuation
 151 $\sqrt{C_m}/M(p_T)_m$.

152 The beam energy dependence of relative dynamical mean transverse momentum fluctuations in pp col-
 153 lisions was studied at lower collision energies by the Split Field Magnet (SFM) detector at the Inter-
 154 section Storage Rings (ISR). The SFM experiment measured relative fluctuations in inclusive pp col-
 155 lisions at $\sqrt{s} = 30.8, 45, 52,$ and 63 GeV [40]. The fluctuations are expressed by the quantity R that
 156 is extracted from the multiplicity dependence of the event-by-event $M(p_T)$ dispersion. The measure
 157 $R = [D(M_{E\text{bE}}(p_T)_k)/M(p_T)]_{n \rightarrow \infty}$ is obtained from an extrapolation of the multiplicity-dependent disper-
 158 sion $D(M_{E\text{bE}}(p_T)_k)$ to infinite multiplicity, normalized by the inclusive mean transverse momentum. It

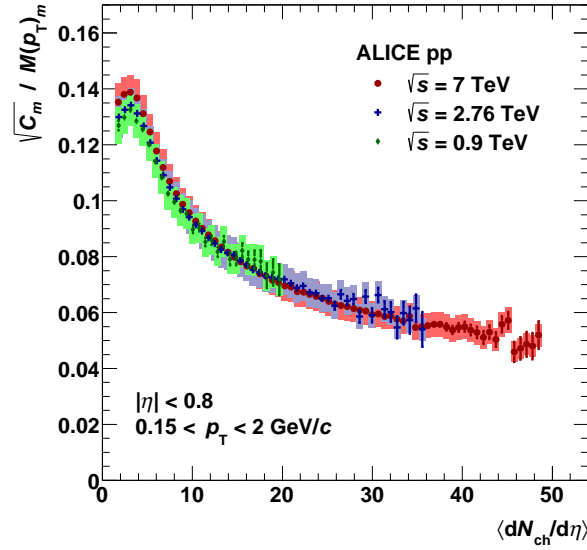


Fig. 1: Relative fluctuation $\sqrt{C_m}/M(p_T)_m$ as a function of $\langle dN_{ch}/d\eta \rangle$ in pp collisions at $\sqrt{s} = 0.9, 2.76$ and 7 TeV.

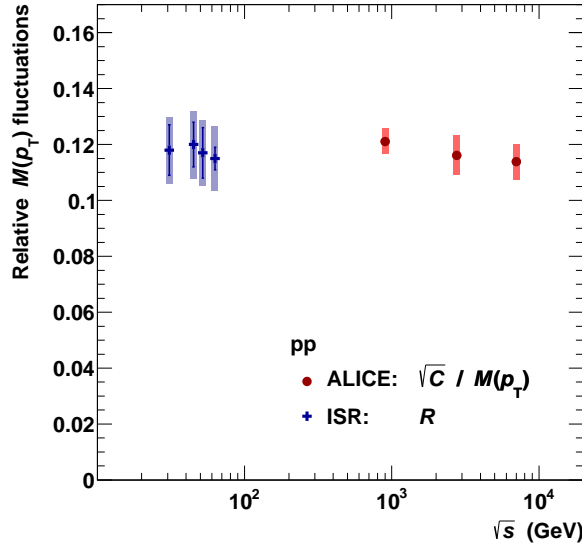


Fig. 2: Relative dynamical mean transverse momentum fluctuations in pp collisions as a function of \sqrt{s} . The ALICE results for $\sqrt{C}/M(p_T)$ are compared to the quantity R measured at the ISR (see text and [40]).

159 is an alternative approach to extract non-statistical transverse momentum fluctuations in inclusive pp
160 collisions.

161 To allow for a comparison to ISR results, an inclusive analysis of ALICE pp data is performed. The
162 relative fluctuation $\sqrt{C}/M(p_T)$ is computed at each collision energy as in (2), however, without subdivi-
163 sion into multiplicity classes m . Monte Carlo studies of pp collisions at $\sqrt{s} = 7$ TeV using PYTHIA8
164 have shown that results for R and $\sqrt{C}/M(p_T)$ agree within 10–15%. The ALICE results for the inclusive
165 $\sqrt{C}/M(p_T)$ as a function of \sqrt{s} are shown in Fig. 2, along with the ISR results for R from [40]. No sig-
166 nificant dependence of the relative transverse momentum fluctuations on the collision energy is observed
167 over this large energy range.

168 The results in pp at $\sqrt{s} = 7$ TeV are compared with results from different event generators. In particular,
169 PYTHIA6 (tunes Perugia-0 and Perugia-11), PYTHIA8.150 and PHOJET have been used.

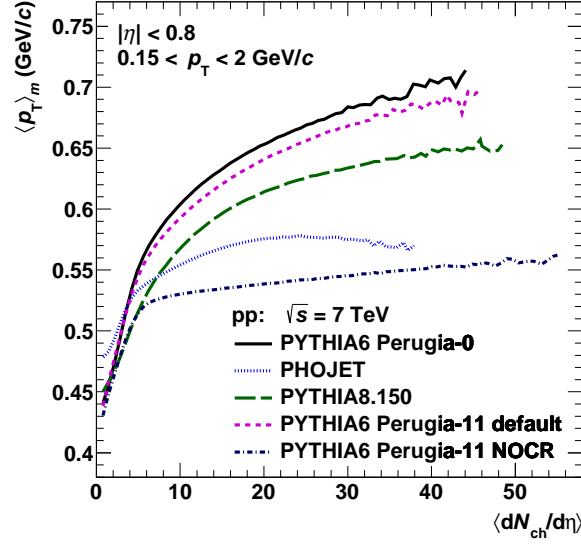


Fig. 3: Results for $\langle p_T \rangle_m$ as a function of $\langle dN_{ch}/d\eta \rangle$ in pp collisions at $\sqrt{s} = 7$ TeV from different event generators.

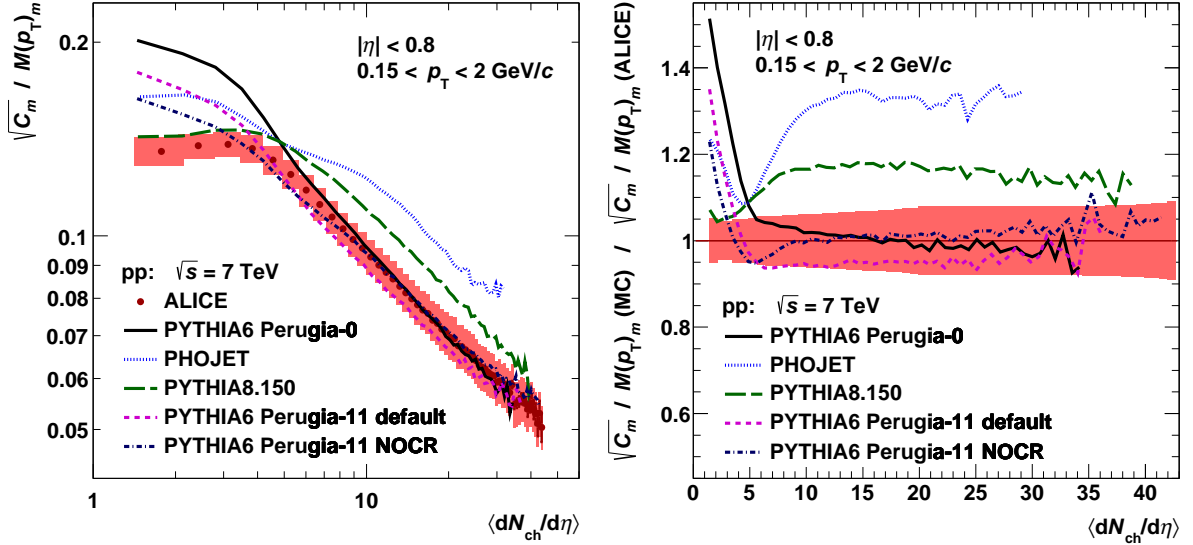


Fig. 4: Left: Relative dynamical fluctuation $\sqrt{C_m}/M(p_T)_m$ for data and different event generators in pp collisions at $\sqrt{s} = 7$ TeV as a function of $\langle dN_{ch}/d\eta \rangle$. Right: Ratio models to data. The red error band indicates the statistical and systematic data uncertainties added in quadrature.

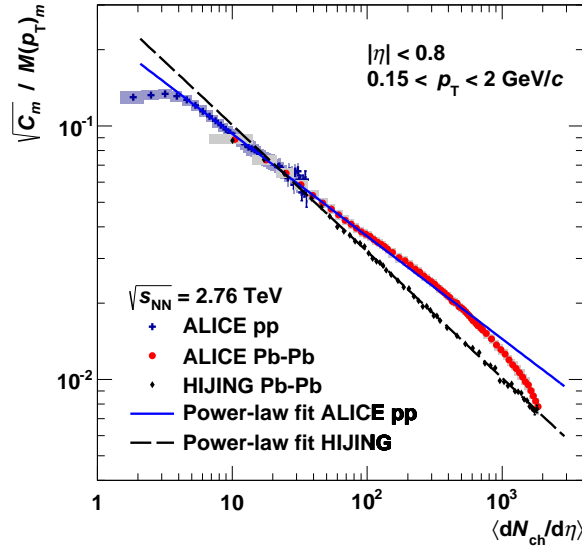


Fig. 5: Relative dynamical fluctuation $\sqrt{C_m}/M(p_T)_m$ as a function of $\langle dN_{ch}/d\eta \rangle$ in pp and Pb–Pb collisions at $\sqrt{s_{NN}} = 2.76$ TeV. Also shown are results from HIJING and power-law fits to pp (solid line) and HIJING (dashed line) (see text).

170 It has been pointed out that high-multiplicity events in pp collisions at LHC energies are driven by multi-
 171 parton interactions (MPIs) [41]. This picture is also suggested by recent studies of the event sphericity
 172 in pp collisions [42]. MPIs are independent processes on the perturbative level. However, the color
 173 reconnection mechanism between produced strings may lead to correlations in the hadronic final state.
 174 Color reconnection is also the driving mechanism in PYTHIA for the increase of $\langle p_T \rangle$ as a function of
 175 N_{ch} [43, 44].

176 The default PYTHIA6 Perugia-11 tune including the color-reconnection mechanism is compared to re-
 177 sults of the same tune without color-reconnection (NOCR). Figure 3 shows model calculations for $\langle p_T \rangle_m$
 178 as a function of $\langle dN_{ch}/d\eta \rangle$ in $0.15 < p_T < 2$ GeV/c and $|\eta| < 0.8$ in pp collisions at $\sqrt{s} = 7$ TeV. The MC
 179 generators yield qualitatively different results for the multiplicity dependence, in particular PHOJET and
 180 the NOCR version of PYTHIA6 Perugia-11 show only little increase of $\langle p_T \rangle_m$ with multiplicity. Good
 181 agreement between PYTHIA8 and ALICE results in pp collisions at $\sqrt{s} = 7$ TeV was demonstrated [44],
 182 albeit in a different η and p_T interval.

183 Results for the relative dynamical fluctuation measure $\sqrt{C_m}/M(p_T)_m$ in pp at $\sqrt{s} = 7$ TeV are compared
 184 to model calculations in Fig. 4. The data exhibit a clear power-law dependence with $\langle dN_{ch}/d\eta \rangle$ except for
 185 very small multiplicities. A power-law fit of $\sqrt{C_m}/M(p_T)_m \propto \langle dN_{ch}/d\eta \rangle^b$ in the interval $5 < \langle dN_{ch}/d\eta \rangle <$
 186 30 yields $b = -0.431 \pm 0.001$ (stat.) ± 0.021 (syst.). The significant deviation of the power-law index
 187 from $b = -0.5$ indicates that the observed multiplicity dependence of $M(p_T)$ fluctuations in pp does not
 188 follow a simple superposition scenario, contrary to what might be expected for independent MPIs. All
 189 PYTHIA tunes under study agree with this finding to the extent that they exhibit a similar power-law
 190 index as the data. This is also true for the NOCR calculation which excludes the color reconnection
 191 mechanism in its present implementation in PYTHIA as a dominant source of correlations beyond the
 192 independent superposition scenario.

193 4 Results in Pb–Pb collisions

194 Results for the relative dynamical fluctuation $\sqrt{C_m}/M(p_T)_m$ in Pb–Pb collisions at $\sqrt{s_{NN}} = 2.76$ TeV
 195 as a function of $\langle dN_{ch}/d\eta \rangle$ are shown in Fig. 5. As for pp collisions, significant dynamical fluctu-

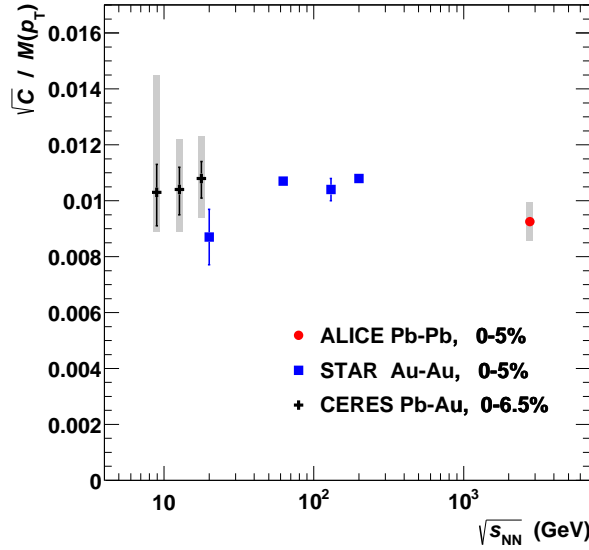


Fig. 6: Mean transverse momentum fluctuations in central heavy-ion collisions as a function of $\sqrt{s_{\text{NN}}}$. The ALICE data point is compared to data from the CERES [13] and STAR [18] experiments. For STAR only statistical uncertainties are available.

196 ations as well as a strong decrease with multiplicity are observed. Also shown in Fig. 5 is the re-
 197 sult of a HIJING [39] simulation (version 1.36) without jet-quenching. A power-law fit in the inter-
 198 val $30 < \langle dN_{\text{ch}}/d\eta \rangle < 1500$ describes the HIJING results very well, except at low multiplicities, and
 199 yields $b = -0.499 \pm 0.003$ (stat.) ± 0.005 (syst.). The approximate $\langle dN_{\text{ch}}/d\eta \rangle^{-0.5}$ scaling reflects the
 200 basic property of HIJING as a superposition model of independent nucleon-nucleon collisions. The
 201 HIJING calculation, in particular the multiplicity dependence, is in obvious disagreement with the data.

202 In peripheral collisions ($\langle dN_{\text{ch}}/d\eta \rangle < 100$), the Pb–Pb results are in very good agreement with the ex-
 203 trapolation of a power-law fit to pp data at $\sqrt{s} = 2.76$ TeV in the interval $5 < \langle dN_{\text{ch}}/d\eta \rangle < 25$, with
 204 $b = -0.405 \pm 0.002$ (stat.) ± 0.036 (syst.). This is remarkable because significant differences in $\langle p_T \rangle$
 205 are observed between pp and Pb–Pb in this multiplicity range [44]. At larger multiplicities, the Pb–Pb re-
 206 sults deviate from the pp extrapolation. An enhancement in $100 < \langle dN_{\text{ch}}/d\eta \rangle < 500$ is followed by a
 207 pronounced decrease at $\langle dN_{\text{ch}}/d\eta \rangle > 500$, corresponding to centralities $< 40\%$, which indicates a strong
 208 reduction of fluctuations towards central collisions.

209 Measurements of mean transverse momentum fluctuations in central A–A collisions at the SPS [13] and
 210 at RHIC [18] are compared to the ALICE result in Fig. 6. As in pp, there is no significant dependence
 211 on $\sqrt{s_{\text{NN}}}$ observed over a wide range of collision energies.

212 Figure 7 shows a comparison of the ALICE results for $\sqrt{\overline{C}_m}/M(p_T)_m$ to measurements in Au–Au colli-
 213 sions at $\sqrt{s_{\text{NN}}} = 200$ GeV by the STAR experiment at RHIC [18]. In the peripheral region, the STAR
 214 data show very similar scaling with $\langle dN_{\text{ch}}/d\eta \rangle$ as the ALICE data, as shown on the left panel of Fig. 7.
 215 Also shown are the fit to pp data at $\sqrt{s} = 2.76$ TeV from Fig. 5 and the result of a power-law fit to the
 216 STAR data in $\langle dN_{\text{ch}}/d\eta \rangle < 200$ where the power is fixed to $b = -0.405$. Good agreement of the ALICE
 217 and STAR data with the fits is observed in peripheral collisions. The decrease of fluctuations in central
 218 collisions is similar in ALICE and STAR, however, no significant enhancement in semi-central events
 219 is observed in the STAR data. In the right panel of Fig. 7, the results for $\sqrt{\overline{C}_m}/M(p_T)_m$ in ALICE and
 220 STAR are shown as a function of the mean number of participating nucleons $\langle N_{\text{part}} \rangle$. In this representa-
 221 tion, the measurements of $\sqrt{\overline{C}_m}/M(p_T)_m$ from ALICE and STAR are compatible within the rather large
 222 experimental uncertainties on $\langle N_{\text{part}} \rangle$ in STAR. A power-law fit $\sqrt{\overline{C}_m}/M(p_T)_m \propto \langle N_{\text{part}} \rangle^b$ to the ALICE
 223 data in the interval $10 < \langle N_{\text{part}} \rangle < 40$ yields $b = -0.472 \pm 0.007$ (stat.) ± 0.037 (syst.). The agreement be-

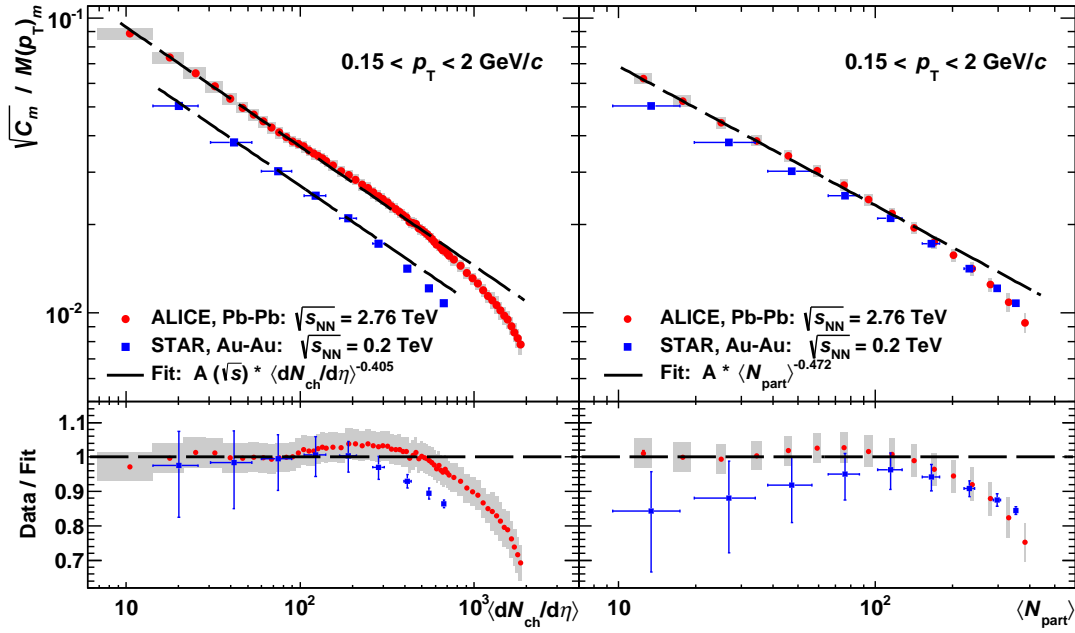


Fig. 7: Left: Relative dynamical fluctuation $\sqrt{C_m}/M(p_T)_m$ as a function of $\langle dN_{ch}/d\eta \rangle$ in Pb–Pb collisions at $\sqrt{s_{NN}} = 2.76$ TeV from ALICE compared to results from STAR in Au–Au collisions at $\sqrt{s_{NN}} = 200$ GeV [18]. Also shown as dashed lines are results from power-law fits to the data (see text). Right: same data as a function of $\langle N_{part} \rangle$.

224 tween ALICE and STAR data as a function of $\langle N_{part} \rangle$ points to a relation between the observed fluctuation
 225 patterns and the collision geometry.

226 Transverse momentum correlations and fluctuations may be modified as a consequence of collective
 227 flow in A–A collisions. It should be noted, however, that event-averaged radial flow and azimuthal
 228 asymmetries are not expected to give rise to strong transverse momentum fluctuations in azimuthally
 229 symmetric detectors [13, 16]. On the other hand, $M(p_T)$ fluctuations may occur due to fluctuating initial
 230 conditions that are also related to event-by-event fluctuations of radial flow and azimuthal asymmetries.
 231 We compare our results to calculations from the AMPT model [45] which has been demonstrated to
 232 give a reasonable description of inclusive and event-averaged bulk properties in Pb–Pb collisions at LHC
 233 energies [46, 47], in particular of the measured elliptic flow coefficient v_2 . Figure 8 shows the ratio of
 234 $\sqrt{C_m}/M(p_T)_m$ in data and models to the result of a fit of $A \cdot \langle dN_{ch}/d\eta \rangle^{-0.5}$ to the HIJING simulation in
 235 the interval $30 < \langle dN_{ch}/d\eta \rangle < 1500$. For $\langle dN_{ch}/d\eta \rangle < 30$, HIJING agrees well with the results from pp
 236 and Pb–Pb. At larger multiplicities, none of the models shows quantitative agreement with the Pb–Pb
 237 data. The default AMPT calculation gives rise to increased fluctuations on top of the underlying HIJING
 238 scenario exceeding those observed in the data, except for very peripheral collisions. In contrast, the
 239 AMPT calculation with string melting, where partons after rescattering are recombined by a hadronic
 240 coalescence scheme, predicts smaller fluctuations. On the other hand, both AMPT versions exhibit a
 241 pronounced fall-off in central collisions which is in qualitative agreement with the data.

242 In a recent approach [24], initial spatial fluctuations of glasma flux tubes have been related to mean
 243 transverse momentum fluctuations of final state hadrons via their coupling to a collective flow field. A
 244 comparison of these calculations to data from ALICE and STAR is shown in [24]. Good agreement is
 245 found in the semi-central and central region, where the data deviate from the pp extrapolation.

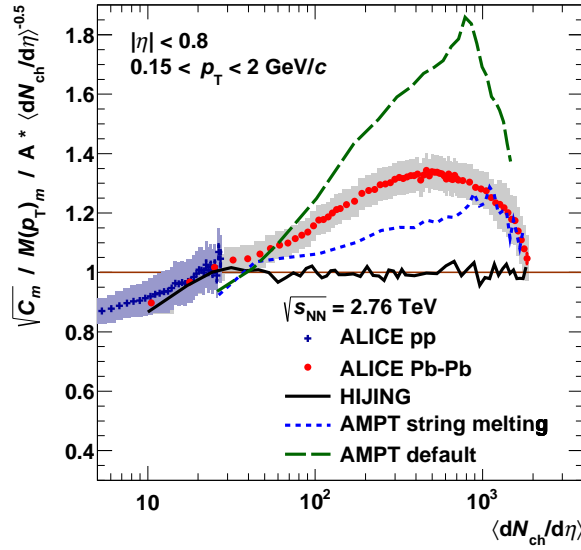


Fig. 8: Relative dynamical fluctuation $\sqrt{C_m}/M(p_T)_m$ normalized to $\langle dN_{ch}/d\eta \rangle^{-0.5}$ (see text) as a function of $\langle dN_{ch}/d\eta \rangle$ in pp and Pb–Pb collisions at $\sqrt{s_{NN}} = 2.76$ TeV. The ALICE data are compared to results from HIJING and AMPT.

246 5 Summary and conclusions

247 First results on event-by-event fluctuations of the mean transverse momentum of charged particles in pp
 248 and Pb–Pb collisions at the LHC are presented. Expressed in terms of the relative dynamical fluctuation
 249 $\sqrt{C_m}/M(p_T)_m$, little energy dependence of the mean transverse momentum fluctuations is observed in
 250 pp at $\sqrt{s} = 0.9, 2.76$ and 7 TeV. The results are also compatible with similar measurements at the ISR.
 251 For the first time, mean transverse momentum fluctuations in pp are studied as a function of $\langle dN_{ch}/d\eta \rangle$.
 252 A characteristic decrease of $\sqrt{C_m}/M(p_T)_m$ following a power law is observed. The decrease is weaker
 253 than expected from a superposition of independent sources. The nature of such sources in pp is subject to
 254 future studies, but a connection to the concept of multi-parton interactions is suggestive. Model studies
 255 using PYTHIA however indicate that there is no strong sensitivity of transverse momentum fluctuations
 256 to the mechanism of color reconnection.

257 In peripheral Pb–Pb collisions ($\langle dN_{ch}/d\eta \rangle < 100$), the dependence of $\sqrt{C_m}/M(p_T)_m$ on $\langle dN_{ch}/d\eta \rangle$ is
 258 very similar to that observed in pp collisions at the corresponding collision energy. At larger multiplici-
 259 ties, the Pb–Pb data deviate significantly from an extrapolation of pp results and show a strong decrease
 260 for $\langle dN_{ch}/d\eta \rangle > 500$. The results for the most central collisions are of the same magnitude as previous
 261 measurements at the SPS and at RHIC. The centrality dependence of $\sqrt{C_m}/M(p_T)_m$ is compatible with
 262 that observed in Au–Au at $\sqrt{s_{NN}} = 200$ GeV.

263 The Pb–Pb data can not be described by models based on independent nucleon-nucleon collisions such
 264 as HIJING. Models which include initial state density fluctuations and their effect on the development
 265 of collectivity in the final state are in qualitative agreement with the data. This suggests a connection
 266 between the observed fluctuations of transverse momentum and azimuthal correlations, and their relation
 267 to fluctuations in the initial state of the collision.

Acknowledgements

The ALICE Collaboration would like to thank all its engineers and technicians for their invaluable contribu-
 tions to the construction of the experiment and the CERN accelerator teams for the outstanding
 performance of the LHC complex.

The ALICE Collaboration gratefully acknowledges the resources and support provided by all Grid centres and the Worldwide LHC Computing Grid (WLCG) collaboration.

The ALICE Collaboration acknowledges the following funding agencies for their support in building and running the ALICE detector:

State Committee of Science, World Federation of Scientists (WFS) and Swiss Fonds Kidagan, Armenia, Conselho Nacional de Desenvolvimento Científico e Tecnológico (CNPq), Financiadora de Estudos e Projetos (FINEP), Fundação de Amparo à Pesquisa do Estado de São Paulo (FAPESP);

National Natural Science Foundation of China (NSFC), the Chinese Ministry of Education (CMOE) and the Ministry of Science and Technology of China (MSTC);

Ministry of Education and Youth of the Czech Republic;

Danish Natural Science Research Council, the Carlsberg Foundation and the Danish National Research Foundation;

The European Research Council under the European Community's Seventh Framework Programme;

Helsinki Institute of Physics and the Academy of Finland;

French CNRS-IN2P3, the 'Region Pays de Loire', 'Region Alsace', 'Region Auvergne' and CEA, France;

German BMBF and the Helmholtz Association;

General Secretariat for Research and Technology, Ministry of Development, Greece;

Hungarian OTKA and National Office for Research and Technology (NKTH);

Department of Atomic Energy and Department of Science and Technology of the Government of India;

Istituto Nazionale di Fisica Nucleare (INFN) and Centro Fermi - Museo Storico della Fisica e Centro Studi e Ricerche "Enrico Fermi", Italy;

MEXT Grant-in-Aid for Specially Promoted Research, Japan;

Joint Institute for Nuclear Research, Dubna;

National Research Foundation of Korea (NRF);

CONACYT, DGAPA, México, ALFA-EC and the EPLANET Program (European Particle Physics Latin American Network)

Stichting voor Fundamenteel Onderzoek der Materie (FOM) and the Nederlandse Organisatie voor Wetenschappelijk Onderzoek (NWO), Netherlands;

Research Council of Norway (NFR);

Polish Ministry of Science and Higher Education;

National Science Centre, Poland;

Ministry of National Education/Institute for Atomic Physics and CNCS-UEFISCDI - Romania;

Ministry of Education and Science of Russian Federation, Russian Academy of Sciences, Russian Federal Agency of Atomic Energy, Russian Federal Agency for Science and Innovations and The Russian Foundation for Basic Research;

Ministry of Education of Slovakia;

Department of Science and Technology, South Africa;

CIEMAT, EELA, Ministerio de Economía y Competitividad (MINECO) of Spain, Xunta de Galicia (Consellería de Educación), CEADEN, Cubaenergía, Cuba, and IAEA (International Atomic Energy Agency);

Swedish Research Council (VR) and Knut & Alice Wallenberg Foundation (KAW);

Ukraine Ministry of Education and Science;

United Kingdom Science and Technology Facilities Council (STFC);

The United States Department of Energy, the United States National Science Foundation, the State of Texas, and the State of Ohio;

Ministry of Science, Education and Sports of Croatia and Unity through Knowledge Fund, Croatia.

References

- [1] S. Jeon and V. Koch, in R.C. Hwa (ed.) et al.: Quark-Gluon-Plasma 430-490. hep-ph/0304012.
- [2] S. Mrówczyński, Phys. Lett. B 314 (1993) 118.
- [3] L. Stodolsky, Phys. Rev. Lett. 75 (1995) 1044.
- [4] E. Shuryak, Phys. Lett. B 423 (1998) 9.
- [5] M.A. Stephanov, K. Rajagopal, E.V. Shuryak, Phys. Rev. Lett. 81 (1998) 4816.
- [6] M.A. Stephanov, K. Rajagopal, E.V. Shuryak Phys. Rev. D 60 (1999) 114028.
- [7] H. Heiselberg, Phys. Rep. 351 (2001) 161.
- [8] A. Dumitru, R. Pisarski, Phys. Lett. B 504 (2001) 282.
- [9] Z. Fodor, S. D. Katz, J. High Energy Phys. 0404 (2004) 050.
- [10] H. Appelshäuser, et al., NA49 Collaboration, Phys. Lett. B 459 (1999) 679.
- [11] D. Adamová, et al., CERES Collaboration, Nucl. Phys. A 727 (2003) 97.
- [12] T. Anticic, et al., NA49 Collaboration, Phys. Rev. C 70 (2004) 034902.
- [13] D. Adamová, et al., CERES Collaboration, Nucl. Phys. A 811 (2008) 179.
- [14] T. Anticic, et al., NA49 Collaboration, Phys. Rev. C 79 (2009) 044904.
- [15] K. Adcox, et al., PHENIX Collaboration, Phys. Rev. C 66 (2002) 024901.
- [16] S.S. Adler, et al., PHENIX Collaboration, Phys. Rev. Lett. 93 (2004) 092301.
- [17] J. Adams et al., STAR Collaboration, Phys. Rev. C 71 (2005) 064906.
- [18] J. Adams et al., STAR Collaboration, Phys. Rev. C 72 (2005) 044902.
- [19] J. Adams et al., STAR Collaboration, J. Phys. G: Nucl. Part. Phys. 32 (2006) L37.
- [20] J. Adams et al., STAR Collaboration, J. Phys. G: Nucl. Part. Phys. 34 (2007) 451.
- [21] E.G. Ferreiro, F. del Moral, C. Pajares, Phys. Rev. C 69 (2004) 034901.
- [22] S. Voloshin, Phys. Lett. B 632 (2006) 490.
- [23] S. Gavin, Phys. Rev. Lett. 92 (2004) 162301.
- [24] S. Gavin, G. Moschelli, Phys. Rev. C 85 (2012) 014905.
- [25] S. Gavin, G. Moschelli, Phys. Rev. C 86 (2012) 034902.
- [26] B. Alver and G. Roland, Phys. Rev. C 81 (2010) 054905.
- [27] L. Evans, P. Bryant (Eds.), JINST 3 (2008) S08001.
- [28] K. Aamodt, et al., ALICE Collaboration, JINST 3 (2008) S08002.
- [29] J. Alme, et al., ALICE Collaboration, Nucl. Instrum. Methods A 622 (2010) 316.
- [30] K. Aamodt et al., ALICE Collaboration, Phys. Rev. Lett. 106 (2011) 032301.
- [31] B. Abelev, et al., ALICE Collaboration, Phys. Rev. C 88 (2013) 044909.
- [32] S.A. Voloshin, V. Koch, H.G. Ritter, Phys. Rev. C 60 (1999) 024901.
- [33] K. Aamodt, et al., ALICE Collaboration, Eur. Phys. J. C 68 (2010) 89.
- [34] R. Brun, et al., CERN program Library Long Write-Up, W5013, GEANT Detector Description and Simulation Tool, 1994.
- [35] R. Brun, et al., ALICE Collaboration, Nucl. Instrum. Methods A 502 (2003) 339.
- [36] T. Sjöstrand, S. Mrenna, P. Skands, JHEP 0605 (2006) 026.
- [37] P.Z. Skands, Phys. Rev. D 82 (2010) 074018.
- [38] R. Engel, J. Ranft, S. Roesler, Phys. Rev. D 52 (1995) 1459.
- [39] W.T. Deng, X.N. Wang, R. Xu, Phys. Lett. B 701 (2011) 133.
- [40] K. Braune, et al., Phys. Lett. B 123 (1983) 467.
- [41] P. Bartalini, et al., arXiv:1111.0469.

- [42] B. Abelev, et al., ALICE Collaboration, Eur. Phys. J. C 72 (2012) 2124.
- [43] T. Sjöstrand, arXiv:1310.8073
- [44] B. Abelev, et al., ALICE Collaboration, Phys. Lett. B 727 (2013) 371.
- [45] Z.W. Lin, C.M. Ko, B. A. Li, B. Zhang, S. Pal, Phys. Rev. C 72 (2005) 064901.
- [46] J. Xu, C.M. Ko, Phys. Rev. C 84 (2011) 014903.
- [47] J. Xu, C.M. Ko, Phys. Rev. C 84 (2011) 044907.

A The ALICE Collaboration

B. Abelev⁷¹, J. Adam³⁷, D. Adamová⁷⁹, M.M. Aggarwal⁸³, G. Aglieri Rinella³⁴, M. Agnello^{107,90}, A. Agostinelli²⁶, N. Agrawal⁴⁴, Z. Ahammed¹²⁶, N. Ahmad¹⁸, I. Ahmed¹⁵, S.U. Ahn⁶⁴, S.A. Ahn⁶⁴, I. Aimo^{90,107}, S. Aiola¹³¹, M. Ajaz¹⁵, A. Akindinov⁵⁴, S.N. Alam¹²⁶, D. Aleksandrov⁹⁶, B. Alessandro¹⁰⁷, D. Alexandre⁹⁸, A. Alici^{101,12}, A. Alkin³, J. Alme³⁵, T. Alt³⁹, S. Altinpinar¹⁷, I. Altsybeev¹²⁵, C. Alves Garcia Prado¹¹⁵, C. Andrei⁷⁴, A. Andronic⁹³, V. Anguelov⁸⁹, J. Anielski⁵⁰, T. Antičić⁹⁴, F. Antinori¹⁰⁴, P. Antonioli¹⁰¹, L. Aphecetche¹⁰⁹, H. Appelshäuser⁴⁹, S. Arcelli²⁶, N. Armesto¹⁶, R. Arnaldi¹⁰⁷, T. Aronsson¹³¹, I.C. Arsene^{93,21}, M. Arslandok⁴⁹, A. Augustinus³⁴, R. Averbeck⁹³, T.C. Awes⁸⁰, M.D. Azmi^{85,18}, M. Bach³⁹, A. Badalà¹⁰³, Y.W. Baek^{66,40}, S. Bagnasco¹⁰⁷, R. Bailhache⁴⁹, R. Bala⁸⁶, A. Baldisseri¹⁴, F. Baltasar Dos Santos Pedrosa³⁴, R.C. Baral⁵⁷, R. Barbera²⁷, F. Barile³¹, G.G. Barnaföldi¹³⁰, L.S. Barnby⁹⁸, V. Barret⁶⁶, J. Bartke¹¹², M. Basile²⁶, N. Bastid⁶⁶, S. Basu¹²⁶, B. Bathen⁵⁰, G. Batigne¹⁰⁹, A. Batista Camejo⁶⁶, B. Batyunya⁶², P.C. Batzing²¹, C. Baumann⁴⁹, I.G. Bearden⁷⁶, H. Beck⁴⁹, C. Bedda⁹⁰, N.K. Behera⁴⁴, I. Belikov⁵¹, F. Bellini²⁶, R. Bellwied¹¹⁷, E. Belmont-Moreno⁶⁰, R. Belmont III¹²⁹, V. Belyaev⁷², G. Bencedi¹³⁰, S. Beole²⁵, I. Berceanu⁷⁴, A. Bercuci⁷⁴, Y. Berdnikov^{ii,81}, D. Berenyi¹³⁰, M.E. Berger⁸⁸, R.A. Bertens⁵³, D. Berzano²⁵, L. Betev³⁴, A. Bhasin⁸⁶, I.R. Bhat⁸⁶, A.K. Bhati⁸³, B. Bhattacharjee⁴¹, J. Bhom¹²², L. Bianchi²⁵, N. Bianchi⁶⁸, C. Bianchin⁵³, J. Bielčik³⁷, J. Bielčiková⁷⁹, A. Bilandzic⁷⁶, S. Bjelogrić⁵³, F. Blanco¹⁰, D. Blau⁹⁶, C. Blume⁴⁹, F. Bock^{89,70}, A. Bogdanov⁷², H. Bøggild⁷⁶, M. Bogolyubsky¹⁰⁸, F.V. Böhmer⁸⁸, L. Boldizsár¹³⁰, M. Bombara³⁸, J. Book⁴⁹, H. Borel¹⁴, A. Borissov^{92,129}, M. Borri⁷⁸, F. Bossú⁶¹, M. Botje⁷⁷, E. Botta²⁵, S. Böttger⁴⁸, P. Braun-Munzinger⁹³, M. Bregant¹¹⁵, T. Breitner⁴⁸, T.A. Broker⁴⁹, T.A. Browning⁹¹, M. Broz³⁷, E. Bruna¹⁰⁷, G.E. Bruno³¹, D. Budnikov⁹⁵, H. Buesching⁴⁹, S. Bufalino¹⁰⁷, P. Buncic³⁴, O. Busch⁸⁹, Z. Buthelezi⁶¹, D. Caffarri^{28,34}, X. Cai⁷, H. Caines¹³¹, L. Calero Diaz⁶⁸, A. Caliva⁵³, E. Calvo Villar⁹⁹, P. Camerini²⁴, F. Carena³⁴, W. Carena³⁴, J. Castillo Castellanos¹⁴, E.A.R. Casula²³, V. Catanescu⁷⁴, C. Cavicchioli³⁴, C. Ceballos Sanchez⁹, J. Cepila³⁷, P. Cerello¹⁰⁷, B. Chang¹¹⁸, S. Chapeland³⁴, J.L. Charvet¹⁴, S. Chattopadhyay¹²⁶, S. Chattopadhyay⁹⁷, V. Chelnokov³, M. Cherney⁸², C. Cheshkov¹²⁴, B. Cheynis¹²⁴, V. Chibante Barroso³⁴, D.D. Chinellato^{116,117}, P. Chochula³⁴, M. Chojnacki⁷⁶, S. Choudhury¹²⁶, P. Christakoglou⁷⁷, C.H. Christensen⁷⁶, P. Christiansen³², T. Chujo¹²², S.U. Chung⁹², C. Cicalo¹⁰², L. Cifarelli^{12,26}, F. Cindolo¹⁰¹, J. Cleymans⁸⁵, F. Colamaria³¹, D. Colella³¹, A. Collu²³, M. Colocci²⁶, G. Conesa Balbastre⁶⁷, Z. Conesa del Valle⁴⁷, M.E. Connors¹³¹, J.G. Contreras^{11,37}, T.M. Cormier^{129,80}, Y. Corrales Morales²⁵, P. Cortese³⁰, I. Cortés Maldonado², M.R. Cosentino¹¹⁵, F. Costa³⁴, P. Crochet⁶⁶, R. Cruz Albino¹¹, E. Cuautle⁵⁹, L. Cunqueiro^{34,68}, A. Dainese¹⁰⁴, R. Dang⁷, A. Danu⁵⁸, D. Das⁹⁷, I. Das⁴⁷, K. Das⁹⁷, S. Das⁴, A. Dash¹¹⁶, S. Dash⁴⁴, S. De¹²⁶, H. Delagrange^{109,i}, A. Deloff⁷³, E. Dénes¹³⁰, G. D'Erasmus³¹, A. De Caro^{29,12}, G. de Cataldo¹⁰⁰, J. de Cuveland³⁹, A. De Falco²³, D. De Gruttola^{12,29}, N. De Marco¹⁰⁷, S. De Pasquale²⁹, R. de Rooij⁵³, M.A. Diaz Corchero¹⁰, T. Dietel^{85,50}, P. Dillenseger⁴⁹, R. Diviá³⁴, D. Di Bari³¹, S. Di Liberto¹⁰⁵, A. Di Mauro³⁴, P. Di Nezza⁶⁸, Ø. Djuvsland¹⁷, A. Dobrin⁵³, T. Dobrowolski⁷³, D. Domenicis Gimenez¹¹⁵, B. Dönigus⁴⁹, O. Dordic²¹, S. Dørheim⁸⁸, A.K. Dubey¹²⁶, A. Dubla⁵³, L. Ducroux¹²⁴, P. Dupieux⁶⁶, A.K. Dutta Majumdar⁹⁷, T. E. Hilden⁴², R.J. Ehlers¹³¹, D. Elia¹⁰⁰, H. Engel⁴⁸, B. Erazmus^{109,34}, H.A. Erdal³⁵, D. Eschweiler³⁹, B. Espagnon⁴⁷, M. Esposito³⁴, M. Estienne¹⁰⁹, S. Esumi¹²², D. Evans⁹⁸, S. Evdokimov¹⁰⁸, D. Fabris¹⁰⁴, J. Faivre⁶⁷, D. Falchieri²⁶, A. Fantoni⁶⁸, M. Fasel^{89,70}, D. Fehlker¹⁷, L. Feldkamp⁵⁰, D. Felea⁵⁸, A. Feliciello¹⁰⁷, G. Feofilov¹²⁵, J. Ferencei⁷⁹, A. Fernández Téllez², E.G. Ferreira¹⁶, A. Ferretti²⁵, A. Festanti²⁸, J. Figiel¹¹², M.A.S. Figueredo¹¹⁹, S. Filchagin⁹⁵, D. Finogeev⁵², F.M. Fionda³¹, E.M. Fiore³¹, E. Floratos⁸⁴, M. Floris³⁴, S. Foertsch⁶¹, P. Foka⁹³, S. Fokin⁹⁶, E. Fragiaco¹⁰⁶, A. Francescon^{28,34}, U. Frankenfeld⁹³, U. Fuchs³⁴, C. Furget⁶⁷, A. Furs⁵², M. Fusco Girard²⁹, J.J. Gaardhøje⁷⁶, M. Gagliardi²⁵, A.M. Gago⁹⁹, M. Gallio²⁵, D.R. Gangadharan^{70,19}, P. Ganoti^{80,84}, C. Gao⁷, C. Garabatos⁹³, E. Garcia-Solis¹³, C. Gargiulo³⁴, I. Garishvili⁷¹, J. Gerhard³⁹, M. Germain¹⁰⁹, A. Gheata³⁴, M. Gheata^{34,58}, B. Ghidini³¹, P. Ghosh¹²⁶, S.K. Ghosh⁴, P. Gianotti⁶⁸, P. Giubellino³⁴, E. Gladysz-Dziadus¹¹², P. Glässel⁸⁹, A. Gomez Ramirez⁴⁸, P. González-Zamora¹⁰, S. Gorbunov³⁹, L. Görlich¹¹², S. Gotovac¹¹¹, L.K. Graczykowski¹²⁸, A. Grelli⁵³, A. Grigoras³⁴, C. Grigoras³⁴, V. Grigoriev⁷², A. Grigoryan¹, S. Grigoryan⁶², B. Grinyov³, N. Grion¹⁰⁶, J.F. Grosse-Oetringhaus³⁴, J.-Y. Grossiord¹²⁴, R. Grosso³⁴, F. Guber⁵², R. Guernane⁶⁷, B. Guerzoni²⁶, M. Guilbaud¹²⁴, K. Gulbrandsen⁷⁶, H. Gulkanyan¹, M. Gumbo⁸⁵, T. Gunji¹²¹, A. Gupta⁸⁶, R. Gupta⁸⁶, K. H. Khan¹⁵, R. Haake⁵⁰, Ø. Haaland¹⁷, C. Hadjidakis⁴⁷, M. Haiduc⁵⁸, H. Hamagaki¹²¹, G. Hamar¹³⁰, L.D. Hanratty⁹⁸, A. Hansen⁷⁶, J.W. Harris¹³¹, H. Hartmann³⁹, A. Harton¹³, D. Hatzifotiadou¹⁰¹, S. Hayashi¹²¹, S.T. Heckel⁴⁹, M. Heide⁵⁰, H. Helstrup³⁵, A. Herghelegiu⁷⁴, G. Herrera Corral¹¹, B.A. Hess³³, K.F. Hetland³⁵, B. Hippolyte⁵¹, J. Hladky⁵⁶, P. Hristov³⁴, M. Huang¹⁷, T.J. Humanic¹⁹, N. Hussain⁴¹, T. Hussain¹⁸, D. Hutter³⁹, D.S. Hwang²⁰, R. Ilkaev⁹⁵, I. Ilkiv⁷³, M. Inaba¹²², G.M. Innocenti²⁵, C. Ionita³⁴,

M. Ippolitov⁹⁶, M. Irfan¹⁸, M. Ivanov⁹³, V. Ivanov⁸¹, A. Jachořkowski²⁷, P.M. Jacobs⁷⁰, C. Jahnke¹¹⁵, H.J. Jang⁶⁴, M.A. Janik¹²⁸, P.H.S.Y. Jayarathna¹¹⁷, C. Jena²⁸, S. Jena¹¹⁷, R.T. Jimenez Bustamante⁵⁹, P.G. Jones⁹⁸, H. Jung⁴⁰, A. Jusko⁹⁸, V. Kadyshchikov⁶², P. Kalinak⁵⁵, A. Kalweit³⁴, J. Kamin⁴⁹, J.H. Kang¹³², V. Kaplin⁷², S. Kar¹²⁶, A. Karasu Uysal⁶⁵, O. Karavichev⁵², T. Karavicheva⁵², E. Karpechev⁵², U. Keschull⁴⁸, R. Keidel¹³³, D.L.D. Keijdener⁵³, M. Keil^{SVN34}, M.M. Khan^{iii.18}, P. Khan⁹⁷, S.A. Khan¹²⁶, A. Khanzadeev⁸¹, Y. Kharlov¹⁰⁸, B. Kileng³⁵, B. Kim¹³², D.W. Kim^{40.64}, D.J. Kim¹¹⁸, J.S. Kim⁴⁰, M. Kim⁴⁰, M. Kim¹³², S. Kim²⁰, T. Kim¹³², S. Kirsch³⁹, I. Kisel³⁹, S. Kiselev⁵⁴, A. Kisiel¹²⁸, G. Kiss¹³⁰, J.L. Klay⁶, J. Klein⁸⁹, C. Klein-Bösing⁵⁰, A. Kluge³⁴, M.L. Knichel⁹³, A.G. Knospe¹¹³, C. Kobdaj^{110.34}, M. Kofarago³⁴, M.K. Köhler⁹³, T. Kollegger³⁹, A. Kolojvari¹²⁵, V. Kondratiev¹²⁵, N. Kondratyeva⁷², A. Konevskikh⁵², V. Kovalenko¹²⁵, M. Kowalski¹¹², S. Kox⁶⁷, G. Koyithatta Meethalevedu⁴⁴, J. Kral¹¹⁸, I. Králik⁵⁵, A. Kravčáková³⁸, M. Krelina³⁷, M. Kretz³⁹, M. Krivda^{55.98}, F. Krizek⁷⁹, E. Kryshen³⁴, M. Krzewicki^{93.39}, V. Kučera⁷⁹, Y. Kucheriaev^{96.i}, T. Kugathasan³⁴, C. Kuhn⁵¹, P.G. Kuijer⁷⁷, I. Kulakov⁴⁹, J. Kumar⁴⁴, P. Kurashvili⁷³, A. Kurepin⁵², A.B. Kurepin⁵², A. Kuryakin⁹⁵, S. Kushpil⁷⁹, M.J. Kweon^{89.46}, Y. Kwon¹³², P. Ladron de Guevara⁵⁹, C. Lagana Fernandes¹¹⁵, I. Lakomov⁴⁷, R. Langoy¹²⁷, C. Lara⁴⁸, A. Lardeux¹⁰⁹, A. Lattuca²⁵, S.L. La Pointe¹⁰⁷, P. La Rocca²⁷, R. Lea²⁴, L. Leardini⁸⁹, G.R. Lee⁹⁸, I. Legrand³⁴, J. Lehnert⁴⁹, R.C. Lemmon⁷⁸, V. Lenti¹⁰⁰, E. Leogrande⁵³, M. Leoncino²⁵, I. León Monzón¹¹⁴, P. Lévai¹³⁰, S. Li^{7.66}, J. Lien¹²⁷, R. Lietava⁹⁸, S. Lindal²¹, V. Lindenstruth³⁹, C. Lippmann⁹³, M.A. Lisa¹⁹, H.M. Ljunggren³², D.F. Lodato⁵³, P.I. Loenne¹⁷, V.R. Loggins¹²⁹, V. Loginov⁷², D. Lohner⁸⁹, C. Loizides⁷⁰, X. Lopez⁶⁶, E. López Torres⁹, X.-G. Lu⁸⁹, P. Luettig⁴⁹, M. Lunardon²⁸, G. Luparello^{53.24}, R. Ma¹³¹, A. Maevskaya⁵², M. Mager³⁴, D.P. Mahapatra⁵⁷, S.M. Mahmood²¹, A. Maire^{51.89}, R.D. Majka¹³¹, M. Malaev⁸¹, I. Maldonado Cervantes⁵⁹, L. Malinina^{iv.62}, D. Mal'Kevich⁵⁴, P. Malzacher⁹³, A. Mamonov⁹⁵, L. Manceau¹⁰⁷, V. Manko⁹⁶, F. Manso⁶⁶, V. Manzari¹⁰⁰, M. Marchisone^{66.25}, J. Mareš⁵⁶, G.V. Margagliotti²⁴, A. Margotti¹⁰¹, A. Marín⁹³, C. Markert^{34.113}, M. Marquard⁴⁹, I. Martashvili¹²⁰, N.A. Martin⁹³, P. Martinengo³⁴, M.I. Martínez², G. Martínez García¹⁰⁹, J. Martin Blanco¹⁰⁹, Y. Martynov³, A. Mas¹⁰⁹, S. Masciocchi⁹³, M. Maserà²⁵, A. Masoni¹⁰², L. Massacrier¹⁰⁹, A. Mastroserio³¹, A. Matyja¹¹², C. Mayer¹¹², J. Mazer¹²⁰, M.A. Mazzoni¹⁰⁵, D. McDonald¹¹⁷, F. Meddi²², A. Menchaca-Rocha⁶⁰, E. Meninno²⁹, J. Mercado Pérez⁸⁹, M. Meres³⁶, Y. Miake¹²², K. Mikhaylov^{54.62}, L. Milano³⁴, J. Milosevic^{v.21}, A. Mischke⁵³, A.N. Mishra⁴⁵, D. Miśkowiec⁹³, J. Mitra¹²⁶, C.M. Mitu⁵⁸, J. Mlynar¹²⁹, N. Mohammadi⁵³, B. Mohanty^{75.126}, L. Molnar⁵¹, L. Montaño Zetina¹¹, E. Montes¹⁰, M. Morando²⁸, D.A. Moreira De Godoy^{115.109}, S. Moretto²⁸, A. Morreale¹⁰⁹, A. Morsch³⁴, V. Muccifora⁶⁸, E. Mudnic¹¹¹, D. Mühlheim⁵⁰, S. Muhuri¹²⁶, M. Mukherjee¹²⁶, H. Müller³⁴, M.G. Munhoz¹¹⁵, S. Murray⁸⁵, L. Musa³⁴, J. Musinsky⁵⁵, B.K. Nandi⁴⁴, R. Nania¹⁰¹, E. Nappi¹⁰⁰, C. Nattrass¹²⁰, K. Nayak⁷⁵, T.K. Nayak¹²⁶, S. Nazarenko⁹⁵, A. Nedosekin⁵⁴, M. Nicassio⁹³, M. Niculescu^{58.34}, J. Niedziela³⁴, B.S. Nielsen⁷⁶, S. Nikolaev⁹⁶, S. Nikulin⁹⁶, V. Nikulin⁸¹, B.S. Nilsen⁸², F. Noferini^{101.12}, P. Nomokonov⁶², G. Nooren⁵³, J. Norman¹¹⁹, A. Nyanin⁹⁶, J. Nystrand¹⁷, H. Oeschler⁸⁹, S. Oh¹³¹, S.K. Oh^{vi.63.40}, A. Okatan⁶⁵, T. Okubo⁴³, L. Olah¹³⁰, J. Oleniacz¹²⁸, A.C. Oliveira Da Silva¹¹⁵, J. Onderwaater⁹³, C. Oppedisano¹⁰⁷, A. Ortiz Velasquez^{32.59}, A. Oskarsson³², J. Otwinowski^{112.93}, K. Oyama⁸⁹, M. Ozdemir⁴⁹, P. Sahoo⁴⁵, Y. Pachmayer⁸⁹, M. Pachr³⁷, P. Pagano²⁹, G. Paic⁵⁹, C. Pajares¹⁶, S.K. Pal¹²⁶, A. Palmeri¹⁰³, D. Pant⁴⁴, V. Papikyan¹, G.S. Pappalardo¹⁰³, P. Pareek⁴⁵, W.J. Park⁹³, S. Parmar⁸³, A. Passfeld⁵⁰, D.I. Patalakha¹⁰⁸, V. Paticchio¹⁰⁰, B. Paul⁹⁷, T. Pawlak¹²⁸, T. Peitzmann⁵³, H. Pereira Da Costa¹⁴, E. Pereira De Oliveira Filho¹¹⁵, D. Peresunko⁹⁶, C.E. Pérez Lara⁷⁷, A. Pesci¹⁰¹, V. Peskov⁴⁹, Y. Pestov⁵, V. Petráček³⁷, M. Petran³⁷, M. Petris⁷⁴, M. Petrovici⁷⁴, C. Petta²⁷, S. Piano¹⁰⁶, M. Pikna³⁶, P. Pillot¹⁰⁹, O. Pinazza^{101.34}, L. Pinsky¹¹⁷, D.B. Piyarathna¹¹⁷, M. Płoskoń⁷⁰, M. Planinic^{94.123}, J. Pluta¹²⁸, S. Pochybova¹³⁰, P.L.M. Podesta-Lerma¹¹⁴, M.G. Poghosyan^{82.34}, E.H.O. Pohjoisaho⁴², B. Polichtchouk¹⁰⁸, N. Poljak^{123.94}, A. Pop⁷⁴, S. Porteboeuf-Houssais⁶⁶, J. Porter⁷⁰, B. Potukuchi⁸⁶, S.K. Prasad^{129.4}, R. Preghenella^{101.12}, F. Prino¹⁰⁷, C.A. Pruneau¹²⁹, I. Pshenichnov⁵², M. Puccio¹⁰⁷, G. Puddu²³, P. Pujahari¹²⁹, V. Punin⁹⁵, J. Putschke¹²⁹, H. Qvigstad²¹, A. Rachevski¹⁰⁶, S. Raha⁴, S. Rajput⁸⁶, J. Rak¹¹⁸, A. Rakotozafindrabe¹⁴, L. Ramello³⁰, R. Raniwala⁸⁷, S. Raniwala⁸⁷, S.S. Räsänen⁴², B.T. Rascanu⁴⁹, D. Rathee⁸³, A.W. Rauf¹⁵, V. Razazi²³, K.F. Read¹²⁰, J.S. Real⁶⁷, K. Redlich^{vii.73}, R.J. Reed^{131.129}, A. Rehman¹⁷, P. Reichelt⁴⁹, M. Reicher⁵³, F. Reidt^{34.89}, R. Renfordt⁴⁹, A.R. Reolon⁶⁸, A. Reshetin⁵², F. Rettig³⁹, J.-P. Revol³⁴, K. Reygers⁸⁹, V. Riabov⁸¹, R.A. Ricci⁶⁹, T. Richert³², M. Richter²¹, P. Riedler³⁴, W. Riegler³⁴, F. Riggi²⁷, A. Rivetti¹⁰⁷, E. Rocco⁵³, M. Rodríguez Cahuantzi², A. Rodríguez Manso⁷⁷, K. Røed²¹, E. Rogochaya⁶², S. Rohni⁸⁶, D. Rohr³⁹, D. Röhrich¹⁷, R. Romita^{78.119}, F. Ronchetti⁶⁸, L. Ronflette¹⁰⁹, P. Rosnet⁶⁶, A. Rossi³⁴, F. Roukoutakis⁸⁴, A. Roy⁴⁵, C. Roy⁵¹, P. Roy⁹⁷, A.J. Rubio Montero¹⁰, R. Rui²⁴, R. Russo²⁵, E. Ryabinkin⁹⁶, Y. Ryabov⁸¹, A. Rybicki¹¹², S. Sadovsky¹⁰⁸, K. Šafařík³⁴, B. Sahlmüller⁴⁹, R. Sahoo⁴⁵, S. Sahoo⁵⁷, P.K. Sahu⁵⁷, J. Saini¹²⁶, S. Sakai⁶⁸, C.A. Salgado¹⁶, J. Salzwedel¹⁹, S. Sambyal⁸⁶, V. Samsonov⁸¹, X. Sanchez Castro⁵¹, F.J. Sánchez Rodríguez¹¹⁴, L. Šándor⁵⁵,

A. Sandoval⁶⁰, M. Sano¹²², G. Santagati²⁷, D. Sarkar¹²⁶, E. Scapparone¹⁰¹, F. Scarlassara²⁸, R.P. Scharenberg⁹¹, C. Schiaua⁷⁴, R. Schicker⁸⁹, C. Schmidt⁹³, H.R. Schmidt³³, S. Schuchmann⁴⁹, J. Schukraft³⁴, M. Schulc³⁷, T. Schuster¹³¹, Y. Schutz^{109,34}, K. Schwarz⁹³, K. Schweda⁹³, G. Scioli²⁶, E. Scomparin¹⁰⁷, R. Scott¹²⁰, G. Segato²⁸, J.E. Seger⁸², Y. Sekiguchi¹²¹, I. Selyuzhenkov⁹³, K. Senosi⁶¹, J. Seo⁹², E. Serradilla^{10,60}, A. Sevcenco⁵⁸, A. Shabetai¹⁰⁹, G. Shabratova⁶², R. Shahoyan³⁴, A. Shangaraev¹⁰⁸, A. Sharma⁸⁶, N. Sharma¹²⁰, S. Sharma⁸⁶, K. Shigaki⁴³, K. Shtejer^{25,9}, Y. Sibirak⁹⁶, S. Siddhanta¹⁰², T. Siemarczuk⁷³, D. Silvermyr⁸⁰, C. Silvestre⁶⁷, G. Simatovic¹²³, R. Singaravelu¹²⁶, R. Singh⁸⁶, S. Singha^{75,126}, V. Singhal¹²⁶, B.C. Sinha¹²⁶, T. Sinha⁹⁷, B. Sitar³⁶, M. Sitta³⁰, T.B. Skaali²¹, K. Skjerdal¹⁷, M. Slupecki¹¹⁸, N. Smirnov¹³¹, R.J.M. Snellings⁵³, C. Sogaard³², R. Soltz⁷¹, J. Song⁹², M. Song¹³², F. Soramel²⁸, S. Sorensen¹²⁰, M. Spacek³⁷, E. Spiriti⁶⁸, I. Sputowska¹¹², M. Spyropoulou-Stassinaki⁸⁴, B.K. Srivastava⁹¹, J. Stachel⁸⁹, I. Stan⁵⁸, G. Stefanek⁷³, M. Steinpreis¹⁹, E. Stenlund³², G. Steyn⁶¹, J.H. Stiller⁸⁹, D. Stocco¹⁰⁹, M. Stolpovskiy¹⁰⁸, P. Strmen³⁶, A.A.P. Suaide¹¹⁵, T. Sugitate⁴³, C. Suire⁴⁷, M. Suleymanov¹⁵, R. Sultanov⁵⁴, M. Šumbera⁷⁹, T.J.M. Symons⁷⁰, A. Szabo³⁶, A. Szanto de Toledo¹¹⁵, I. Szarka³⁶, A. Szczepankiewicz³⁴, M. Szymanski¹²⁸, J. Takahashi¹¹⁶, M.A. Tangaro³¹, J.D. Tapia Takaki^{viii,47}, A. Tarantola Peloni⁴⁹, A. Tarazona Martinez³⁴, M. Tariq¹⁸, M.G. Tarczila⁷⁴, A. Tauro³⁴, G. Tejeda Muñoz², A. Telesca³⁴, K. Terasaki¹²¹, C. Terrevoli²³, J. Thäder⁹³, D. Thomas⁵³, R. Tieulent¹²⁴, A.R. Timmins¹¹⁷, A. Toia^{49,104}, V. Trubnikov³, W.H. Trzaska¹¹⁸, T. Tsuji¹²¹, A. Tumkin⁹⁵, R. Turrisi¹⁰⁴, T.S. Tveter²¹, K. Ullaland¹⁷, A. Uras¹²⁴, G.L. Usai²³, M. Vajzer⁷⁹, M. Vala^{55,62}, L. Valencia Palomo⁶⁶, S. Vallero^{25,89}, P. Vande Vyvre³⁴, J. Van Der Maarel⁵³, J.W. Van Hoorne³⁴, M. van Leeuwen⁵³, A. Vargas², M. Vargyas¹¹⁸, R. Varma⁴⁴, M. Vasileiou⁸⁴, A. Vasiliev⁹⁶, V. Vechernin¹²⁵, M. Veldhoen⁵³, A. Velure¹⁷, M. Venaruzzo^{69,24}, E. Vercellin²⁵, S. Vergara Limón², R. Vernet⁸, M. Verweij¹²⁹, L. Vickovic¹¹¹, G. Viesti²⁸, J. Viinikainen¹¹⁸, Z. Vilakazi⁶¹, O. Villalobos Baillie⁹⁸, A. Vinogradov⁹⁶, L. Vinogradov¹²⁵, Y. Vinogradov⁹⁵, T. Virgili²⁹, V. Vislavicius³², Y.P. Viyogi¹²⁶, A. Vodopyanov⁶², M.A. Völkl⁸⁹, K. Voloshin⁵⁴, S.A. Voloshin¹²⁹, G. Volpe³⁴, B. von Haller³⁴, I. Vorobyev¹²⁵, D. Vranic^{34,93}, J. Vrláková³⁸, B. Vulpescu⁶⁶, A. Vyushin⁹⁵, B. Wagner¹⁷, J. Wagner⁹³, V. Wagner³⁷, M. Wang^{7,109}, Y. Wang⁸⁹, D. Watanabe¹²², M. Weber^{34,117}, S.G. Weber⁹³, J.P. Wessels⁵⁰, U. Westerhoff⁵⁰, J. Wiechula³³, J. Wikne²¹, M. Wilde⁵⁰, G. Wilk⁷³, J. Wilkinson⁸⁹, M.C.S. Williams¹⁰¹, B. Windelband⁸⁹, M. Winn⁸⁹, C.G. Yaldo¹²⁹, Y. Yamaguchi¹²¹, H. Yang⁵³, P. Yang⁷, S. Yang¹⁷, S. Yano⁴³, S. Yasnopolskiy⁹⁶, J. Yi⁹², Z. Yin⁷, I.-K. Yoo⁹², I. Yushmanov⁹⁶, A. Zaborowska¹²⁸, V. Zaccaro⁷⁶, C. Zach³⁷, A. Zaman¹⁵, C. Zampolli¹⁰¹, S. Zaporozhets⁶², A. Zarochentsev¹²⁵, P. Závada⁵⁶, N. Zaviyalov⁹⁵, H. Zbroszczyk¹²⁸, I.S. Zgura⁵⁸, M. Zhalov⁸¹, H. Zhang⁷, X. Zhang^{7,70}, Y. Zhang⁷, C. Zhao²¹, N. Zhigareva⁵⁴, D. Zhou⁷, F. Zhou⁷, Y. Zhou⁵³, Zhou, Zhuo¹⁷, H. Zhu⁷, J. Zhu^{109,7}, X. Zhu⁷, A. Zichichi^{26,12}, A. Zimmermann⁸⁹, M.B. Zimmermann^{34,50}, G. Zinovjev³, Y. Zoccarato¹²⁴, M. Zyzak⁴⁹

Affiliation notes

- ⁱ Deceased
- ⁱⁱ Also at: St. Petersburg State Polytechnical University
- ⁱⁱⁱ Also at: Department of Applied Physics, Aligarh Muslim University, Aligarh, India
- ^{iv} Also at: M.V. Lomonosov Moscow State University, D.V. Skobeltsyn Institute of Nuclear Physics, Moscow, Russia
- ^v Also at: University of Belgrade, Faculty of Physics and "Vinča" Institute of Nuclear Sciences, Belgrade, Serbia
- ^{vi} Permanent Address: Permanent Address: Konkuk University, Seoul, Korea
- ^{vii} Also at: Institute of Theoretical Physics, University of Wrocław, Wrocław, Poland
- ^{viii} Also at: University of Kansas, Lawrence, KS, United States

Collaboration Institutes

- ¹ A.I. Alikhanyan National Science Laboratory (Yerevan Physics Institute) Foundation, Yerevan, Armenia
- ² Benemérita Universidad Autónoma de Puebla, Puebla, Mexico
- ³ Bogolyubov Institute for Theoretical Physics, Kiev, Ukraine
- ⁴ Bose Institute, Department of Physics and Centre for Astroparticle Physics and Space Science (CAPSS), Kolkata, India
- ⁵ Budker Institute for Nuclear Physics, Novosibirsk, Russia
- ⁶ California Polytechnic State University, San Luis Obispo, CA, United States
- ⁷ Central China Normal University, Wuhan, China

- 8 Centre de Calcul de l'IN2P3, Villeurbanne, France
- 9 Centro de Aplicaciones Tecnológicas y Desarrollo Nuclear (CEADEN), Havana, Cuba
- 10 Centro de Investigaciones Energéticas Medioambientales y Tecnológicas (CIEMAT), Madrid, Spain
- 11 Centro de Investigación y de Estudios Avanzados (CINVESTAV), Mexico City and Mérida, Mexico
- 12 Centro Fermi - Museo Storico della Fisica e Centro Studi e Ricerche "Enrico Fermi", Rome, Italy
- 13 Chicago State University, Chicago, USA
- 14 Commissariat à l'Energie Atomique, IRFU, Saclay, France
- 15 COMSATS Institute of Information Technology (CIIT), Islamabad, Pakistan
- 16 Departamento de Física de Partículas and IGFAE, Universidad de Santiago de Compostela, Santiago de Compostela, Spain
- 17 Department of Physics and Technology, University of Bergen, Bergen, Norway
- 18 Department of Physics, Aligarh Muslim University, Aligarh, India
- 19 Department of Physics, Ohio State University, Columbus, OH, United States
- 20 Department of Physics, Sejong University, Seoul, South Korea
- 21 Department of Physics, University of Oslo, Oslo, Norway
- 22 Dipartimento di Fisica dell'Università 'La Sapienza' and Sezione INFN Rome, Italy
- 23 Dipartimento di Fisica dell'Università and Sezione INFN, Cagliari, Italy
- 24 Dipartimento di Fisica dell'Università and Sezione INFN, Trieste, Italy
- 25 Dipartimento di Fisica dell'Università and Sezione INFN, Turin, Italy
- 26 Dipartimento di Fisica e Astronomia dell'Università and Sezione INFN, Bologna, Italy
- 27 Dipartimento di Fisica e Astronomia dell'Università and Sezione INFN, Catania, Italy
- 28 Dipartimento di Fisica e Astronomia dell'Università and Sezione INFN, Padova, Italy
- 29 Dipartimento di Fisica 'E.R. Caianiello' dell'Università and Gruppo Collegato INFN, Salerno, Italy
- 30 Dipartimento di Scienze e Innovazione Tecnologica dell'Università del Piemonte Orientale and Gruppo Collegato INFN, Alessandria, Italy
- 31 Dipartimento Interateneo di Fisica 'M. Merlin' and Sezione INFN, Bari, Italy
- 32 Division of Experimental High Energy Physics, University of Lund, Lund, Sweden
- 33 Eberhard Karls Universität Tübingen, Tübingen, Germany
- 34 European Organization for Nuclear Research (CERN), Geneva, Switzerland
- 35 Faculty of Engineering, Bergen University College, Bergen, Norway
- 36 Faculty of Mathematics, Physics and Informatics, Comenius University, Bratislava, Slovakia
- 37 Faculty of Nuclear Sciences and Physical Engineering, Czech Technical University in Prague, Prague, Czech Republic
- 38 Faculty of Science, P.J. Šafárik University, Košice, Slovakia
- 39 Frankfurt Institute for Advanced Studies, Johann Wolfgang Goethe-Universität Frankfurt, Frankfurt, Germany
- 40 Gangneung-Wonju National University, Gangneung, South Korea
- 41 Gauhati University, Department of Physics, Guwahati, India
- 42 Helsinki Institute of Physics (HIP), Helsinki, Finland
- 43 Hiroshima University, Hiroshima, Japan
- 44 Indian Institute of Technology Bombay (IIT), Mumbai, India
- 45 Indian Institute of Technology Indore, Indore (IITI), India
- 46 Inha University, Incheon, South Korea
- 47 Institut de Physique Nucléaire d'Orsay (IPNO), Université Paris-Sud, CNRS-IN2P3, Orsay, France
- 48 Institut für Informatik, Johann Wolfgang Goethe-Universität Frankfurt, Frankfurt, Germany
- 49 Institut für Kernphysik, Johann Wolfgang Goethe-Universität Frankfurt, Frankfurt, Germany
- 50 Institut für Kernphysik, Westfälische Wilhelms-Universität Münster, Münster, Germany
- 51 Institut Pluridisciplinaire Hubert Curien (IPHC), Université de Strasbourg, CNRS-IN2P3, Strasbourg, France
- 52 Institute for Nuclear Research, Academy of Sciences, Moscow, Russia
- 53 Institute for Subatomic Physics of Utrecht University, Utrecht, Netherlands
- 54 Institute for Theoretical and Experimental Physics, Moscow, Russia
- 55 Institute of Experimental Physics, Slovak Academy of Sciences, Košice, Slovakia
- 56 Institute of Physics, Academy of Sciences of the Czech Republic, Prague, Czech Republic
- 57 Institute of Physics, Bhubaneswar, India
- 58 Institute of Space Science (ISS), Bucharest, Romania

- 59 Instituto de Ciencias Nucleares, Universidad Nacional Autónoma de México, Mexico City, Mexico
- 60 Instituto de Física, Universidad Nacional Autónoma de México, Mexico City, Mexico
- 61 iThemba LABS, National Research Foundation, Somerset West, South Africa
- 62 Joint Institute for Nuclear Research (JINR), Dubna, Russia
- 63 Konkuk University, Seoul, South Korea
- 64 Korea Institute of Science and Technology Information, Daejeon, South Korea
- 65 KTO Karatay University, Konya, Turkey
- 66 Laboratoire de Physique Corpusculaire (LPC), Clermont Université, Université Blaise Pascal, CNRS-IN2P3, Clermont-Ferrand, France
- 67 Laboratoire de Physique Subatomique et de Cosmologie, Université Grenoble-Alpes, CNRS-IN2P3, Grenoble, France
- 68 Laboratori Nazionali di Frascati, INFN, Frascati, Italy
- 69 Laboratori Nazionali di Legnaro, INFN, Legnaro, Italy
- 70 Lawrence Berkeley National Laboratory, Berkeley, CA, United States
- 71 Lawrence Livermore National Laboratory, Livermore, CA, United States
- 72 Moscow Engineering Physics Institute, Moscow, Russia
- 73 National Centre for Nuclear Studies, Warsaw, Poland
- 74 National Institute for Physics and Nuclear Engineering, Bucharest, Romania
- 75 National Institute of Science Education and Research, Bhubaneswar, India
- 76 Niels Bohr Institute, University of Copenhagen, Copenhagen, Denmark
- 77 Nikhef, National Institute for Subatomic Physics, Amsterdam, Netherlands
- 78 Nuclear Physics Group, STFC Daresbury Laboratory, Daresbury, United Kingdom
- 79 Nuclear Physics Institute, Academy of Sciences of the Czech Republic, Řež u Prahy, Czech Republic
- 80 Oak Ridge National Laboratory, Oak Ridge, TN, United States
- 81 Petersburg Nuclear Physics Institute, Gatchina, Russia
- 82 Physics Department, Creighton University, Omaha, NE, United States
- 83 Physics Department, Panjab University, Chandigarh, India
- 84 Physics Department, University of Athens, Athens, Greece
- 85 Physics Department, University of Cape Town, Cape Town, South Africa
- 86 Physics Department, University of Jammu, Jammu, India
- 87 Physics Department, University of Rajasthan, Jaipur, India
- 88 Physik Department, Technische Universität München, Munich, Germany
- 89 Physikalisches Institut, Ruprecht-Karls-Universität Heidelberg, Heidelberg, Germany
- 90 Politecnico di Torino, Turin, Italy
- 91 Purdue University, West Lafayette, IN, United States
- 92 Pusan National University, Pusan, South Korea
- 93 Research Division and ExtreMe Matter Institute EMMI, GSI Helmholtzzentrum für Schwerionenforschung, Darmstadt, Germany
- 94 Rudjer Bošković Institute, Zagreb, Croatia
- 95 Russian Federal Nuclear Center (VNIIEF), Sarov, Russia
- 96 Russian Research Centre Kurchatov Institute, Moscow, Russia
- 97 Saha Institute of Nuclear Physics, Kolkata, India
- 98 School of Physics and Astronomy, University of Birmingham, Birmingham, United Kingdom
- 99 Sección Física, Departamento de Ciencias, Pontificia Universidad Católica del Perú, Lima, Peru
- 100 Sezione INFN, Bari, Italy
- 101 Sezione INFN, Bologna, Italy
- 102 Sezione INFN, Cagliari, Italy
- 103 Sezione INFN, Catania, Italy
- 104 Sezione INFN, Padova, Italy
- 105 Sezione INFN, Rome, Italy
- 106 Sezione INFN, Trieste, Italy
- 107 Sezione INFN, Turin, Italy
- 108 SSC IHEP of NRC Kurchatov institute, Protvino, Russia
- 109 SUBATECH, Ecole des Mines de Nantes, Université de Nantes, CNRS-IN2P3, Nantes, France
- 110 Suranaree University of Technology, Nakhon Ratchasima, Thailand
- 111 Technical University of Split FESB, Split, Croatia

- 112 The Henryk Niewodniczanski Institute of Nuclear Physics, Polish Academy of Sciences, Cracow, Poland
- 113 The University of Texas at Austin, Physics Department, Austin, TX, USA
- 114 Universidad Autónoma de Sinaloa, Culiacán, Mexico
- 115 Universidade de São Paulo (USP), São Paulo, Brazil
- 116 Universidade Estadual de Campinas (UNICAMP), Campinas, Brazil
- 117 University of Houston, Houston, TX, United States
- 118 University of Jyväskylä, Jyväskylä, Finland
- 119 University of Liverpool, Liverpool, United Kingdom
- 120 University of Tennessee, Knoxville, TN, United States
- 121 University of Tokyo, Tokyo, Japan
- 122 University of Tsukuba, Tsukuba, Japan
- 123 University of Zagreb, Zagreb, Croatia
- 124 Université de Lyon, Université Lyon 1, CNRS/IN2P3, IPN-Lyon, Villeurbanne, France
- 125 V. Fock Institute for Physics, St. Petersburg State University, St. Petersburg, Russia
- 126 Variable Energy Cyclotron Centre, Kolkata, India
- 127 Vestfold University College, Tonsberg, Norway
- 128 Warsaw University of Technology, Warsaw, Poland
- 129 Wayne State University, Detroit, MI, United States
- 130 Wigner Research Centre for Physics, Hungarian Academy of Sciences, Budapest, Hungary
- 131 Yale University, New Haven, CT, United States
- 132 Yonsei University, Seoul, South Korea
- 133 Zentrum für Technologietransfer und Telekommunikation (ZTT), Fachhochschule Worms, Worms, Germany